A cubic B-spline collocation method for numerically solving fractional diffusion equations used in modelling dye-sensitized solar cells

B. Maldon[1] B. P. Lamichhane[2] N. Thamwattana[3]

(Received 30 September 2020; revised 27 July 2021)

Abstract

As part of the third generation of solar cells, dye-sensitized solar cells (DSSCs) are a novel, cost effective solution to the renewable energy problem. Mathematical modelling provides unique insight into operating DSSCs efficiently, particularly in the role of diffusion in the nanoporous semiconductor of the device. A recently published fractional diffusion model explores the link between the electron density of DSSCs and the porosity of the semiconductor. In this article, we solve the fractional diffusion model numerically using cubic B-splines to discretise space and an implicit finite difference scheme to discretise time. We compute the error by a standard collocation method.

DOI:10.21914/anziamproc.v62.15883 Published 2026-08-26, as part of the Proceedings of the 19th Biennial Computational Techniques and Applications Conference. ISSN 1445-8810. (Print two pages per sheet of paper.)

Contents

1 Introduction

Dye-sensitized solar cells (DSSCs) were originally proposed by O'Regan and Grätzel [19] in 1991. They remain a financially advantageous alternative to traditional silicon based solar cells due primarily to the use of the significantly cheaper nanoporous titanium dioxide (TiO_2).

Södergren et al. [21] developed the first diffusion-based mathematical model for DSSCs, employing an ordinary differential equation to capture electron density in DSSCs. Extensions to this model included time-dependence by Cao et al. [4], nonlinear diffusion by Anta et al. [2] and Maldon et al. [15], and a system of linear diffusion equations that include the electrolyte couple by Andrade et al. [1] and Maldon and Thamwattana [14].

Fractional diffusion offers a unique perspective on the electron diffusion for DSSCs. Nelson [17] and Benkstein et al. [3] studied electron behaviour in TiO_2 under continuous-time random walk (CTRW) simulations, which were used by Maldon and Thamwattana [13] to create a fractional diffusion equation based on Henry and Wearne's model [10].

In this article, we consider the Caputo fractional derivative [5]

$$\frac{d^\gamma f}{dt^\gamma} = \frac{1}{\Gamma(1-\gamma)} \int_0^t \frac{f'(\sigma)}{(t-\sigma)^\gamma}\, d\sigma\,. \tag{1}$$

Given a DSSC of thickness d, let $x = 0$ denote the transparent conductive oxide (TCO) end of the DSSC and $x = d$ denote the counter electrode. The electron density $n(x,t)$ at position $x \in [0,d]$ and time $t \geq 0$ satisfies the fractional partial differential equation (FPDE) [13, for further details]

$$\frac{\partial n}{\partial t} = D_0 \frac{\partial^{1-\gamma}}{\partial t^{1-\gamma}} \frac{\partial^2 n}{\partial x^2} + \varphi \alpha e^{-\alpha x} - k_R[n(x,t) - n_{eq}]\,, \tag{2}$$

where D_0 is the diffusion coefficient, γ is the exponent in the mean square displacement in the CTRW simulation of the semiconductor, φ is the incident photon flux, α is the dye absorption coefficient, k_R is the recombination constant, and n_{eq} is the dark equilibrium electron density. We prescribe the boundary conditions

$$n(0,t) = n_0 := n_{eq} e^{\frac{qV_B}{m_I k_B T}}\,, \tag{3}$$

$$\left.\frac{\partial n}{\partial x}\right|_{x=d} = 0\,, \tag{4}$$

$$n(x,0) = n_0\,, \tag{5}$$

where q is the electron charge, V_B is the bias voltage, m_I is the diode ideality factor, k_B is Boltzmann's constant and T is the temperature of the DSSC. The special case $\gamma = 1$ recovers the standard diffusion special case [10] studied by Maldon et al. [12].

We nondimensionalise equation (2) with the scaling

$$N = \frac{n - n_0}{n_0}\,, \quad \chi = \frac{x}{d}\,, \quad \tau = \left(\frac{D_0}{d^2}\right)^{\frac{1}{\gamma}} t\,.$$

This nondimensionalisation requires the diffusion coefficient D_0 to assume the units $m^2\,s^{-\gamma}$. In the absence of measured fractional diffusion coefficients for DSSCs we use the linear diffusion coefficient value given in Table 2. The nondimensional FPDE is

$$\frac{\partial N}{\partial \tau} = \frac{\partial^{1-\gamma}}{\partial \tau^{1-\gamma}} \frac{\partial^2 N}{\partial \chi^2} + \mu e^{-\nu\chi} - \zeta\left(N + \frac{n_0 - n_{eq}}{n_0}\right), \tag{6}$$

where

$$\mu = \frac{\varphi\alpha}{n_0}\left(\frac{d^2}{D_0}\right)^{\frac{1}{\gamma}}, \quad \nu = \alpha d, \quad \zeta = \frac{k_R}{n_0}\left(\frac{d^2}{D_0}\right)^{\frac{1}{\gamma}}.$$

The nondimensional boundary conditions are

$$N(0,\tau) = 0, \tag{7}$$

$$\left.\frac{\partial N}{\partial \chi}\right|_{\chi=1} = 0, \tag{8}$$

$$N(\chi,0) = 0. \tag{9}$$

In this article, we apply a cubic B-spline collocation method to solve the FPDE (6) under (7), (8) and (9). We calculate the accuracy of the numerical solution with the maximum relative error using an interpolated fine-grid simulation as a pseudo-exact solution.

2 Cubic B-spline collocation method

We solve equation (6) under (7), (8) and (9) using a B-spline collocation method. El Danaf [6] developed a spline method for a space-time fractional diffusion problem with arbitrary Dirichlet boundary conditions. Esen et al. [7] provided a quadratic B-spline method for solving space-time fractional diffusion problems. Zahra and Elkholy [22] also solved fractional ordinary differential equations numerically using cubic spline methods. In this article we use the cubic B-spline functions proposed by Mittal and Jain [16] to

discretise space and the finite difference approximation given by Oldham and Spanier [20] to discretise time.

Let $t_f > 0$ be the (dimensional) final simulation time. The corresponding nondimensional final simulation time is $T_f = \left(D_0/d^2\right)^{1/\gamma} t_f$. Discretise $[0, T_f]$ into N_t temporal nodes and $[0, 1]$ into N_x spatial nodes. Let $(\Delta\chi) = 1/(N_x - 1)$, $(\Delta\tau) = T_f/(N_t - 1)$, $\chi_k = (k-1)(\Delta\chi)$ and $\tau_m = (m-1)(\Delta\tau)$ for each $k = 1, \ldots, N_x$ and $m = 1, \ldots, N_t$.

2.1 Temporal discretisation

To estimate the fractional derivative of a function f with respect to t of order $1-\gamma$ for $0 < \gamma \leq 1$ we use the first order approximation [7, 20]

$$\left.\frac{d^{1-\gamma} f}{d\tau^{1-\gamma}}\right|_{\tau=\tau_m} \approx \frac{(\Delta\tau)^{\gamma-1}}{\Gamma(\gamma+1)} \sum_{p=0}^{m-2} \left[(p+1)^{\gamma} - p^{\gamma}\right] \left[f(\tau_{m-p}) - f(\tau_{m-p-1})\right], \quad (10)$$

where the denominator is the usual Gamma function

$$\Gamma(z) = \int_0^{\infty} x^{z-1} e^{-x}\, dx\,.$$

2.2 Spatial discretisation

At each $\tau = \tau_m$ we estimate the numerical solution to equation (6) with

$$N(\chi, \tau_m) \approx \sum_{j=0}^{N_x+1} \xi_{m,j} B_j(\chi)\,, \quad (11)$$

Table 1: Values of the B-spline functions and their derivatives at key node values, for $j = 0, \ldots, N_x + 1$ [16].

Function	χ_{j-2}	χ_{j-1}	χ_j	χ_{j+1}	χ_{j+2}
$B_j(\chi)$	0	1	4	1	0
$B_j'(\chi)$	0	$3/(\Delta\chi)$	0	$-3/(\Delta\chi)$	0
$B_j''(\chi)$	0	$6/(\Delta\chi)^2$	$-12/(\Delta\chi)^2$	$6/(\Delta\chi)^2$	0

where $\xi_{m,j}$ are the unknown coefficients, and the cubic B-spline functions are [16]

$$B_j(\chi) = \frac{1}{(\Delta\chi)^3} \begin{cases} (\chi - \chi_{j-2})^3 & \chi_{j-2} \le \chi < \chi_{j-1}\,, \\ (\chi - \chi_{j-2})^3 - 4(\chi - \chi_{j-1})^3 & \chi_{j-1} \le \chi < \chi_j\,, \\ (\chi_{j+2} - \chi)^3 - 4(\chi_{j+1} - \chi)^3 & \chi_j \le \chi < \chi_{j+1}\,, \\ (\chi_{j+2} - \chi)^3 & \chi_{j+1} \le \chi < \chi_{j+2}\,, \\ 0 & \text{otherwise,} \end{cases}$$

where we have extended the spatial discretisation to include the ghost nodes χ_{-2}, χ_{-1}, χ_{N_x+2} and χ_{N_x+3}. The spline functions are only evaluated within the domain $[0, 1]$ during the numerical simuation. The values of the spline functions and their derivatives at each relevant spatial node are given in Table 1 [16].

2.3 Implicit finite difference scheme

To satisfy the boundary conditions (7) and (8) we use Table 1 to set

$$\xi_{m,0} + 4\xi_{m,1} + \xi_{m,2} = 0\,,$$
$$\xi_{m,N_x-1} - \xi_{m,N_x+1} = 0\,,$$

for all $m = 1, \ldots, N_t$. To satisfy the initial condition (9), for each $k = 1, \ldots, N_x$ we set the collocation

$$\sum_{j=0}^{N_x+1} \xi_{1,j} B_j(x_k) = N(x_k, 0)\,,$$

which implies $\xi_{1,j} = 0$ for each $j = 1, \ldots, N_x + 1$. For each $m = 2, \ldots, N_t$ and $k = 1, \ldots, N_x$, we set

$$\sum_{j=0}^{N_x+1} \frac{\xi_{m,j} - \xi_{m-1,j}}{(\Delta\tau)} B_j(x_k) =$$
$$\frac{(\Delta\tau)^{\gamma-1}}{\Gamma(\gamma+1)} \sum_{j=0}^{N_x+1} \left(\sum_{p=0}^{m-2} \left[(p+1)^{\gamma} - p^{\gamma} \right] \left[\xi_{m-p,j} - \xi_{m-p-1,j} \right] \right) \left. \frac{d^2 B_j}{dx^2} \right|_{x=x_k}$$
$$+ \mu e^{-\nu x_k} - \zeta \left(\sum_{j=0}^{Nx+1} \xi_{m,j} B_j(x_k) + \frac{n_0 - n_{eq}}{n_0} \right),$$

which, along with the boundary conditions, results in a system of $N_x + 2$ equations in $N_x + 2$ unknowns. For each $m = 2, \ldots, N_t$ we solve the system

$$A\xi_m = R\,,$$

where

$$\xi_m = (\xi_{m,0}, \xi_{m,1}, \ldots, \xi_{m,N_x+1})\,, \tag{12}$$

sparse matrix A has elements

$$A_{1,1} = 1\,, \quad A_{1,2} = 4\,, \quad A_{1,3} = 1\,,$$
$$A_{j,j-1} = 1 + \zeta(\Delta\tau) - \frac{6(\Delta\tau)^{\gamma}}{\Gamma(\gamma+1)(\Delta\chi)^2}\,,$$
$$A_{j,j} = 4(1 + \zeta(\Delta\tau)) + \frac{12(\Delta\tau)^{\gamma}}{\Gamma(\gamma+1)(\Delta\chi)^2}\,,$$
$$A_{j,j+1} = 1 + \zeta(\Delta\tau) - \frac{6(\Delta\tau)^{\gamma}}{\Gamma(\gamma+1)(\Delta\chi)^2}\,,$$

$$A_{N_x+2,N_x} = 1\,, \quad A_{N_x+2,N_x+2} = -1\,,$$

and R is the vector with components $R_1 = 0$, $R_{N_x+2} = 0$ and

$$\begin{aligned} R_j &= \xi_{m-1,j-2} + 4\xi_{m-1,j-1} + \xi_{m-1,j} + (\Delta\tau)\left(\mu e^{-\nu x_{j-1}} - \zeta\frac{n_0 - n_{eq}}{n_0}\right) \\ &- \frac{6(\Delta\tau)^\gamma}{\Gamma(\gamma+1)(\Delta\chi)^2}\left[\xi_{m-1,j-2} - 2\xi_{m-1,j-1} + \xi_{m-1,j}\right] \\ &+ \frac{6(\Delta\tau)^\gamma}{\Gamma(\gamma+1)(\Delta\chi)^2}\sum_{p=1}^{m-2}\left[(p+1)^\gamma - p^\gamma\right]\left[\xi_{m-p,j-2} - 2\xi_{m-p,j-1} + \xi_{m-p,j}\right] \\ &- \frac{6(\Delta\tau)^\gamma}{\Gamma(\gamma+1)(\Delta\chi)^2}\sum_{p=1}^{m-2}\left[(p+1)^\gamma - p^\gamma\right]\left[\xi_{m-p-1,j-2} - 2\xi_{m-p-1,j-1} + \xi_{m-p-1,j}\right], \end{aligned}$$

where $j = 2, \ldots, N_x + 1$. To recover the numerical solution to the original boundary value problem, we calculate

$$n(x, t_m) \approx n_0\left(1 + \sum_{j=0}^{N_x+1}\xi_{m,j}B_j(\chi)\right), \tag{13}$$

where $t_m = \left(D_0/d^2\right)^{-1/\gamma}\tau_m$ is the dimensional time step and $\chi = x/d$ is the nondimensional space variable.

3 Results

To solve equation (2) numerically we use the parameter values in Table 2.

Figure 1 shows the numerical solution to equation (6) under (7), (8) and (9) using the data from Table 2, $N_x = 100$, $N_t = 100$ and $t_f = 1\,s$. From Figure 1 we see the electron density assumes its shape from the interaction of the Dirichlet boundary condition, the exponential source term and diffusion. The electron density grows rapidly from its initial condition, particularly near $\chi = 0$. Given that the Dirichlet boundary condition (7) prescribes a

Table 2: Parameter values for the DSSC model.

Parameter	Value	Unit	Reference
γ	0.612	-	[3]
D_0	10^{-11}	$m^2\,s^{-\gamma}$	[2]
α	10^5	m^{-1}	[8]
d	5×10^{-5}	m	[2]
k_R	4×10^{-8}	s^{-1}	[2]
n_{eq}	10^{22}	m^{-3}	[18]
φ	10^{21}	$m^{-2}\,s^{-1}$	[9]
V_B	0	V	-
μ	8.28×10^7	-	-
ν	5	-	-
ζ	3.31×10^{-26}	-	-

comparatively lower density at $\chi = 0$, the diffusion term creates a peak that moves slowly towards $\chi = 1$ before disappearing in the long term steady-state.

To elucidate the effect of γ on the electron density, Figure 2 plots the numerical solution of equation (6) at $t = 1000\,s$ using the parameter data in Table 2 with $N_x = 100$, $N_t = 100$ and several values of γ. Figure 2 reveals that lower values of γ lead to a slower diffusion process and a higher overall density. In particular, at $t = 1000\,s$ we see that the electron density for the special cases $\gamma = 1$ and $\gamma = 0.75$ have slowed growth compared to the cases for lower values of γ. These densities are in agreement with the numerical results obtained by Maldon and Thamwattana [13], who used an explicit finite difference method.

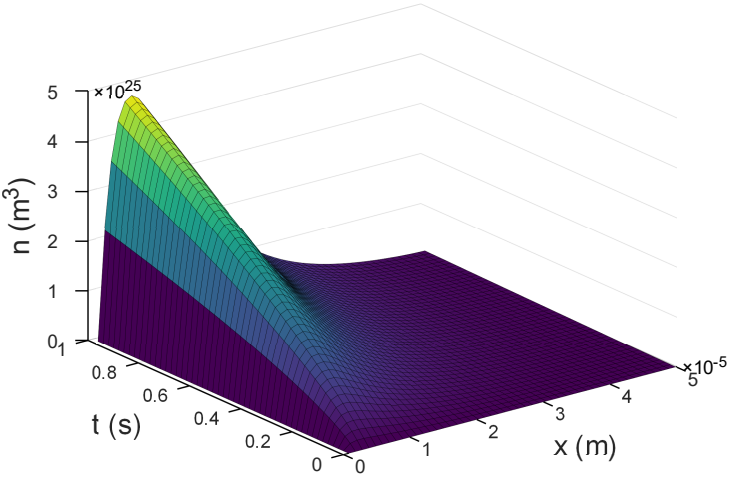

Figure 1: Plot of the numerical solution to equation (6) under (7), (8) and (9) with $N_x = 100$, $N_t = 100$, $t_f = 1\,s$ and $\gamma = 0.612$.

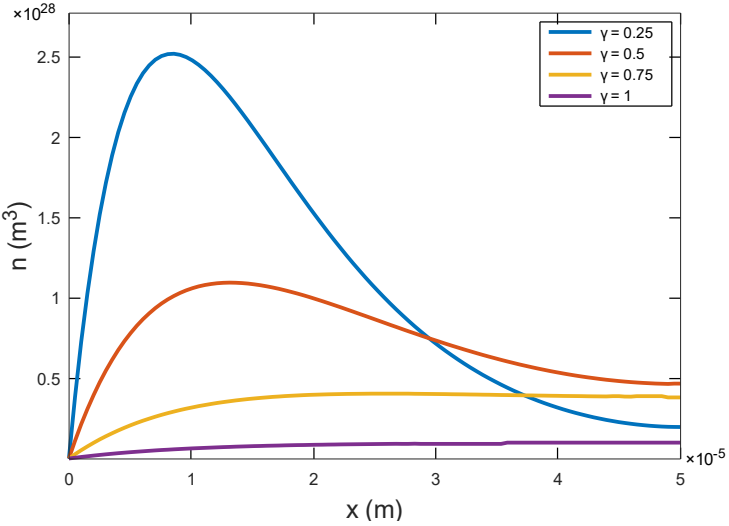

Figure 2: Plot of the numerical solution to equation (6) under (7), (8) and (9) with $N_x = 100$, $N_t = 100$, $t_f = 1000\,s$ and $\gamma = 0.25, 0.5, 0.75$ and $\gamma = 1$.

Table 3: Values for error ϵ for the numerical solution of equation (6) under the data in Table 2, $t_f = 1$, $N_t = 100$, and various values of N_x.

N_x	8	16	32	64
ϵ	2.6468	0.5560	0.1037	0.0085

Table 4: Values for error ϵ for the numerical solution of equation (6) under the data in Table 2, $t_f = 1$, $N_x = 100$, and various values of N_t.

N_t	8	16	32	64
ϵ	0.3462	0.1616	0.0749	0.0310

4 Error calculation

To validate the accuracy of the collocation method we compare to a fine-grid solution that serves as a pseudo-exact solution. Given a solution vector u_c computed on a grid with spatial and temporal step sizes $(\Delta\chi)$ and $(\Delta\tau)$, respectively, and an interpolated fine-grid solution vector u_f, the error is given by

$$\epsilon = \sqrt{(\Delta\chi)(\Delta\tau)}\|u_f - u_c\|, \tag{14}$$

where $\|\cdot\|$ denotes MATLAB's usual norm function.

To calculate the errors we simulate under $t_f = 1$, the data in Table 2 and a fine-grid solution u_f computed with $N_x = 5000$ and $N_t = 5000$. The errors under spatial and temporal refinement are given in Tables 3 and 4, respectively. From Table 3 we see that doubling the number of spatial nodes N_x reduces the error by a factor greater than four, which is consistent with the second order accuracy offered by the cubic B-spline discretisation for a nonlinear fractional diffusion equation in the norm defined by (14) [11]. From Table 4 we see that doubling the number of temporal nodes N_t reduces the error by a factor slightly greater than two, which is consistent with first order approximations.

5 Summary

We solve the fractional partial differential equation (2) using a cubic B-spline collocation method to discretise space and an implicit finite difference method to discretise time. From Figures 1 and 2 we see the solution profile bears a similar shape to the $\gamma = 1$ special case, and lower values of γ lead to higher overall densities and a slower overall diffusion process. The B-spline collocation method gives good agreement with other solutions to equation (2) in the literature. The implicit finite difference method also provides an unconditionally stable temporal discretisation.

Acknowledgements This research has been conducted with the support of the Australian Government Research Training Program Scholarship. The authors are grateful to the Australian Research Council for the funding of Discovery Project DP170102705.

References

[1] L. Andrade, J. Sousa, H. A. Ribeiro, and A. Mendes. "Phenomenological modeling of dye-sensitized solar cells under transient conditions". In: *Solar Energy* 85.5 (2011), pp. 781–793. DOI: 10.1016/j.solener.2011.01.014 (cit. on p. C274).

[2] J. A. Anta, F. Casanueva, and G. Oskam. "A numerical model for charge transport and recombination in dye-sensitized solar cells". In: *J. Phys. Chem. B* 110.11 (2006), pp. 5372–5378. DOI: 10.1021/jp056493h (cit. on pp. C274, C281).

[3] K. D. Benkstein, N. Kopidakis, J. van de Lagemaat, and A. J. Frank. "Influence of the percolation network geometry on electron transport in dye-sensitized titanium dioxide solar cells". In: *J. Phys. Chem. B* 107.31 (2003), pp. 7759–7767. DOI: 10.1021/jp0226811 (cit. on pp. C274, C281).

[4] F. Cao, G. Oskam, G. J. Meyer, and P. C. Searson. “Electron transport in porous nanocrystalline TiO_2 photoelectrochemical cells”. In: *J. Phys. Chem.* 100.42 (1996), pp. 17021–17027. DOI: 10.1021/jp9616573 (cit. on p. C274).

[5] M. Caputo. “Linear models of dissipation whose Q is almost frequency independent—II”. In: *Geophys. J. Int.* 13.5 (1967), pp. 529–539. DOI: 10.1111/j.1365-246X.1967.tb02303.x (cit. on p. C275).

[6] T. S. El Danaf. “Numerical solution for the linear time and space fractional diffusion equation”. In: *J. Vib. Control* 21.9 (2015), pp. 1769–1777. DOI: 10.1177/1077546313500687 (cit. on p. C276).

[7] A. Esen, Y. Ucar, N. Yagmurlu, and O. Tasbozan. “A Galerkin finite element method to solve fractional diffusion and fractional diffusion-wave equations”. In: *Math. Mod. Anal.* 18 (2013), pp. 260–273. DOI: 10.3846/13926292.2013.783884 (cit. on pp. C276, C277).

[8] Y. Gacemi, A. Cheknane, and H. S. Hilal. “Simulation and modelling of charge transport in dye-sensitized solar cells based on carbon nano-tube electrodes”. In: *Physica Scripta* 87.3, 035703 (2013). DOI: 10.1088/0031-8949/87/03/035703 (cit. on p. C281).

[9] R. Gómez and P. Salvador. “Photovoltage dependence on film thickness and type of illumination in nanoporous thin flim electrodes according to a simple diffusion model”. In: *Solar Energy Mat. Solar Cells* 88.4 (2005), pp. 377–388. DOI: 10.1016/j.solmat.2004.11.008 (cit. on p. C281).

[10] B. I. Henry and S. L. Wearne. “Fractional reaction-diffusion”. In: *Physica A* 276 (2000), pp. 448–455. DOI: 10.1016/S0378-4371(99)00469-0 (cit. on pp. C274, C275).

[11] N. Khalid, M. Abbas, M. K. Iqbal, and D. Baleanu. “A numerical investigation of Caputo time fractional Allen–Cahn equation using refined cubic B-spline functions”. In: *Adv. Diff. Eq.* 2020, 158 (2020). DOI: 10.1186/s13662-020-02616-x (cit. on p. C283).

[12] B. Maldon, B. P. Lamichhane, and N. Thamwattana. "Numerical solutions for nonlinear partial differential equations arising from modelling dye-sensitized solar cells". In: *Proceedings of the 18th Biennial Computational Techniques and Applications Conference, CTAC-2018*. Ed. by B. Lamichhane, T. Tran, and J. Bunder. Vol. 60. ANZIAM J. 2019, pp. C231–C246. DOI: 10.21914/anziamj.v60i0.14053 (cit. on p. C275).

[13] B. Maldon and N. Thamwattana. "A fractional diffusion model for dye-sensitized solar cells". In: *Molecules* 25 (2020), pp. 2966–2975. DOI: 10.3390/molecules25132966 (cit. on pp. C274, C275, C281).

[14] B. Maldon and N. Thamwattana. "An analytical solution for charge carrier densities in dye-sensitized solar cells". In: *J. Photochem. Photobio. A* 370 (2019), pp. 41–50. DOI: 10.1016/j.jphotochem.2018.10.018 (cit. on p. C274).

[15] B. Maldon, N. Thamwattana, and M. Edwards. "Exploring nonlinear diffusion equations for modelling dye-sensitized solar cells". In: *Entropy* 22 (2020), p. 248. DOI: 10.3390/e22020248 (cit. on p. C274).

[16] R. C. Mittal and R. K. Jain. "Cubic B-splines collocation method for solving nonlinear parabolic partial differential equations with Neumann boundary conditions". In: *Comm. Nonlin. Sci. Numer. Sim.* 17 (2012), pp. 4616–4625. DOI: 10.1016/j.cnsns.2012.05.007 (cit. on pp. C276, C278).

[17] J. Nelson. "Continuous-time random-walk model of electron transport in nanocrystalline TiO_2 electrodes". In: *Phys. Rev. B* 59.23 (1999), pp. 15374–15380. DOI: 10.1103/PhysRevB.59.15374 (cit. on p. C274).

[18] M. Ni, M. K. H. Leung, D. Y. C. Leung, and K. Sumathy. "An analytical study of the porosity effect on dye-sensitized solar cell performance". In: *Solar Energy Mat. Solar Cells* 90.9 (2006), pp. 1331–1344. DOI: 10.1016/j.solmat.2005.08.006 (cit. on p. C281).

[19] B. O'Regan and M. Grätzel. "A low-cost, high-efficiency solar cell based on dye-sensitized colloidal TiO_2 films". In: *Nature* 353 (1991), pp. 737–740. DOI: 10.1038/353737a0 (cit. on p. C274).

[20] K. Oldham and J. Spanier. *The fractional calculus: Theory and applications of differentiation and integration to arbitrary order*. Vol. III. Elsevier, 1974. URL: https://www.sciencedirect.com/bookseries/mathematics-in-science-and-engineering/vol/111/suppl/C (cit. on p. C277).

[21] S. Södergren, A. Hagfeldt, J. Olsson, and S.-E. Lindquist. "Theoretical models for the action spectrum and the current-voltage characteristics of microporous semiconductor films in electrochemical cells". In: *J. Phys. Chem.* 98 (1994), pp. 5552–5556. DOI: 10.1021/J100072A023 (cit. on p. C274).

[22] W. K. Zahra and S. M. Elkholy. "The use of cubic splines in the numerical solution of fractional differential equations". In: *Int. J. Math. Math. Sci.* 2012, 638026 (2012). DOI: 10.1155/2012/638026 (cit. on p. C276).

Author addresses

1. **B. Maldon**, School of Computer and Information Sciences, University of Newcastle, New South Wales 2308, AUSTRALIA.
mailto:benjamin.maldon@uon.edu.au
orcid:0000-0001-8746-7575

2. **B. P. Lamichhane**, School of Computer and Information Sciences, University of Newcastle, New South Wales 2308, AUSTRALIA.

3. **N. Thamwattana**, School of Computer and Information Sciences, University of Newcastle, New South Wales 2308, AUSTRALIA.